

# DEVELOPMENT OF A HIGHLY SENSITIVE CURRENT AND POSITION MONITOR WITH HTS SQUIDS AND AN HTS MAGNETIC SHIELD

T. Watanabe\*, T. Ikeda, M. Kase, Y. Yano, RIKEN, Wako, Saitama, Japan  
 S. Watanabe, Center for Nuclear Study (CNS), University of Tokyo, Wako, Saitama, Japan  
 Y. Sasaki, Matsushita Electric Industrial, Osaka, Japan  
 T. Kawaguchi, KT Science Ltd., Kakogawa, Hyogo, Japan

## Abstract

A highly sensitive current and position monitor with HTS (High-Temperature Superconducting) SQUIDS (Superconducting QUantum Interference Device) and an HTS magnetic shield for the measurement of the intensity of faint beams, such as a radioisotope beam, has been developed for the RIKEN RI beam factory project. The HTS magnetic shield and the HTS current sensor including the HTS SQUID are cooled by a low-vibration pulse-tube refrigerator. Both the HTS magnetic shield and the HTS current sensor were fabricated by dip-coating a thin  $\text{Bi}_2\text{-Sr}_2\text{-Ca}_2\text{-Cu}_3\text{-O}_x$  (Bi-2223) layer on 99.9% MgO ceramic substrates. The HTS technology enables us to develop a system equipped with a downsized and highly sensitive current monitor. Recently, a prototype system was completed and installed in the beam transport line of the RIKEN Ring Cyclotron to measure the DC-current of high-energy heavy-ion beams. As a result, we succeeded in measuring the intensity of the 600 nA  ${}_{40}\text{Ar}^{17+}$  beam (95 MeV/u). We describe the present status of the monitor system and the results of the beam measurements.

## PRINCIPLE OF HTS SQUID MONITOR

In principle, the SQUID monitor is based on the Meissner effect of superconducting materials. A schematic drawing of the current sensor of the HTS SQUID monitor is shown in Fig. 1 (a). The MgO ceramic tube used as the substrate of the HTS magnetic shield is coated on both sides, inside and outside, with a thin layer (300  $\mu\text{m}$ ) of HTS material. When a charged particle (ion or electron) beam passes along the axis of the HTS tube, a shielding current produced by the Meissner effect flows in the opposite direction along the wall of the HTS tube so as to screen the magnetic field generated by the beam. Since the outer surface is designed to have a bridge circuit (Fig. 1 (a)), the current generated by the charged particle beam concentrates in the bridge circuit and forms an azimuthal magnetic field  $\Phi$  around the bridge circuit. The HTS SQUID is set close to the bridge circuit and can detect the azimuthal magnetic field with a high  $S/N$  ratio. In particular, since the SQUID gradiometer has two pickup coils that are wound in opposite directions and connected in series, the signal level is expected to be improved by a factor of 2, while the background noise can then be significantly reduced, by more

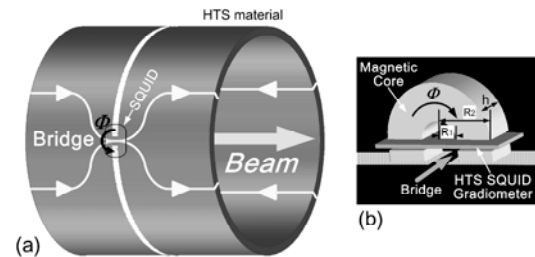


Figure 1: (a) Schematic drawing of the current sensor of the HTS SQUID monitor. (b) Structure consisting of the SQUID gradiometer and the magnetic core near the bridge.

than 40 dB. Furthermore, to obtain a higher coupling efficiency, we are investigating the possibility of introducing a high-permeability magnetic core in the HTS monitor. The sketch (Fig. 1 (b)) represents a structure consisting of the SQUID gradiometer and the magnetic core near the bridge.

## EQUIPMENT

### HTS SQUID system

The HTS DC SQUID system, which is composed of an HTS SQUID gradiometer ( $\text{Y-Ba}_2\text{-Cu}_3\text{O}_{7-\delta}$ ) [1], a cryogenic cable, a flux-locked loop module, a fiber-optic composite cable that connects the flux-locked loop module to the control electronics, and a set of control electronics, is commercially available [2]. Figure 2 shows the circuit diagram of the HTS DC SQUID (2 Josephson junctions) and flux-locked loop. The sensor package (hatched region) in the box is kept below the critical temperature  $T_c$ . The magnetic flux density  $B$  induced by the charged particle beam is transferred to the HTS SQUID with the aid of the pickup coil and the input coil, which are built into the HTS SQUID itself. The flux-locked loop enables linear operation with

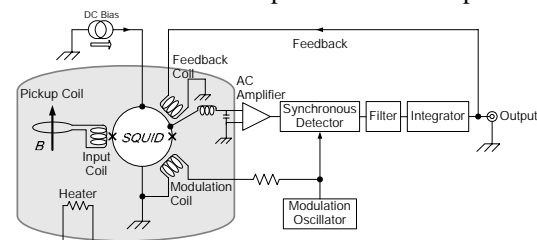


Figure 2: Circuit diagram of the HTS DC SQUID (2 Josephson junctions) and flux-locked loop. The sensor package (hatched region) in the box is kept below the critical temperature  $T_c$ .

\* wtamaki@riken.jp

Table 1: Specifications of the HTS DC SQUID system.

Noise level	34 fT/cm/ $\sqrt{Hz}$ @ 5kHz
Operation temperature	77 K
Feedback gain	1, 2, 5, 10, 20, 50, 100, 200, 500
High-pass filter	DC, 0.3 Hz
Low-pass filter	5 Hz, 500 Hz, 5 kHz, 25 kHz
Data accuracy (AD)	16 bit
Data acquisition rates	20000 words/s
Remote control	IEEE-488, RS-232

respect to the HTS SQUID circuit because it cancels the external magnetic flux density  $B$  by using the feedback coil, as shown in Figure 2. This circuit is composed of a DC bias source, a modulation oscillator and a synchronous detector which are used to create a flux-locked loop circuit, a filter and an integrator. A heater is mounted close to the SQUID in the sensor package in order to purge any magnetic flux trapped in the sensor. A fiber-optic composite cable is used to eliminate grounding and shielding problems that often affect SQUID electronics. The specifications of the system are tabulated in Table 1. The HTS SQUID gradiometer is composed of an input coil and a SQUID loop which has two Josephson junctions (Figure 3 (a)). Figure 3 (b) shows the measured noise spectrum in the frequency domain indicates a  $1/f$  noise structure. White noise is quite low compared with the case of using a conventional HTS SQUID, in which the white noise is over  $1 \text{ pT/cm}/\sqrt{Hz}$ . The coefficient of the magnetic field and the output voltage of the SQUID gradiometer is  $2.43 \text{ nT/V}$  when the maximum gain of 500 is selected.

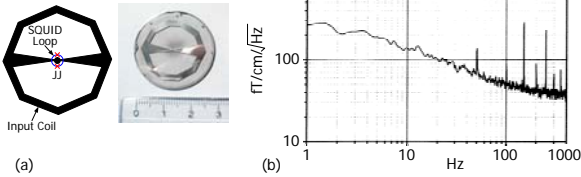


Figure 3: (a) Schematic drawing and picture of the HTS SQUID gradiometer. (b) Measured noise spectrum in frequency domain indicates a  $1/f$  noise structure.

### HTS and permalloy shields

A cylindrical  $\text{Bi}_2\text{-Sr}_2\text{-Ca}_2\text{-Cu}_3\text{-O}_x$  (Bi-2223) HTS magnetic shield (148 mm diameter and 250 mm length) was fabricated by dip-coating ( $300 \mu\text{m}$ ) on a 99.9 % MgO ceramic substrate. An HTS magnetic shield has an advantage in that the magnetic shielding effect is independent of the frequency of environmental magnetic noise, even in the low-frequency band [3]. The critical current ( $I_c$ ) of  $4500 \text{ A/cm}^2$  and the critical temperature ( $T_c$ ) of 106 K of the Bi-2223 cylindrical HTS shield were obtained by a DC four-probe method using a small sample of Bi-2223. In order to measure the field distribution inside the HTS shield and to obtain the attenuation factors, we constructed a measurement system [4]. The system is composed of an X-Y-Z stage driven by stepping motors, a G10-rod which is fixed on the X-Y-Z stage and attached to two HTS-SQUID

probes, a  $\text{LN}_2$  Dewar vessel and a Helmholtz coil that supplies an external field. Hereafter, we define the direction of the cylindrical axis as the  $z$ -direction and the direction perpendicular to the axis as the  $r$ -direction. If the external fields  $B_{z0}$  and  $B_{r0}$  exist, the attenuation factors  $S_z(z)$  and  $S_r(z)$  are defined as

$$S_z(z) = B_z(z)/B_{z0},$$

$$S_r(z) = B_r(z)/B_{r0},$$

where  $B_z(z)$  and  $B_r(z)$  are the  $z$  and  $r$  components of the magnetic field at position  $z$ , respectively. On the basis of the measurement results, the attenuation factors of  $S_z(0) = 5 \times 10^{-4}$  and  $S_r(0) = 8 \times 10^{-2}$  were obtained where the external magnetic field  $B_0$  ( $3.5 \mu\text{T}$ , 1 Hz) was applied. Because the attenuation factor of  $S_r(0)$  of the HTS magnetic shield is inadequate, we undertook to reinforce the HTS magnetic shield. On the basis of various calculations using the finite element method program OPERA-3d [5], three sections of permalloy shields, permalloy 1, permalloy 2 (disk) and permalloy 2 (cylinder), were constructed around the HTS shield. In order to confirm the shielding effect of the reinforced system, a measurement was carried out. A field of  $10^{-5} \text{ T}$  produced by a Helmholtz coil was attenuated to  $10^{-11} \text{ T}$ , which was measured by the SQUID. A strong magnetic shielding system having the attenuation factor of  $10^{-6}$  was obtained [6].

### The HTS SQUID monitor system

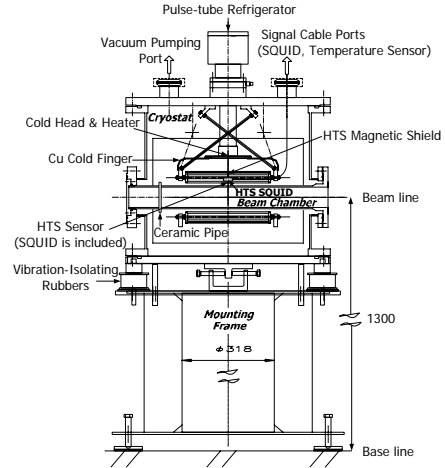


Figure 4: Schematic drawing of the SQUID current monitor system.

A schematic drawing of the HTS SQUID monitor system [7] is shown in Figure 4. The HTS magnetic shield and the HTS current sensor including the HTS SQUID are cooled by a low-vibration pulse-tube refrigerator which has a refrigeration power of 11 W at a temperature of 77 K. The operation temperature can be set in the range between 64 K and 90 K (the critical temperature of the HTS SQUID) using a heater, since the pulse-tube refrigerator is capable of cooling the system to a temperature lower than the temperature of liquid nitrogen. Furthermore, it is possible to stabilize the temperature of the HTS SQUID with an accuracy of 5 mK using a PID feedback controller which has

four thermometers and a heater. We measured the temperature of the cold head as a function of time. Consequently, the standard deviation of the temperature over a period of 18 hours was 3.4 mK.

## RESULTS OF ION BEAM TEST OF HTS SQUID MONITOR

Prior to the ion beam test, we carried out an off-line test. In order to investigate noise sources, not only the vibration originating from the ground but also that generated by the pulse-tube refrigerator itself were analyzed using accelerometers and an FFT, in the time and frequency domains. We calculated the eigenfrequency of the HTS SQUID monitor and selected eight vibration-isolating rubbers (see Figure 4) which can damp the vibration excited by the pulse-tube refrigerator, whose pumping frequency is 5.5 Hz, and there was no problem due to vibration. As a result, the amplitude of the vibration was found to be within  $6 \mu\text{m}$ . Next, the first output signal was observed by feeding a  $1 \mu\text{A}$  sine wave (3 Hz) into a Cu rod which was set in the beam chamber. We confirmed that the measured beam current is not dependent on the beam position or beam radius, by changing the position and the radius of the Cu rod. Furthermore, the output voltage of the SQUID electronics as a function of the simulated beam current is plotted in Figure 5. The dynamic range of 100 dB (from  $1 \mu\text{A}$  to 0.1 A) was obtained by changing the feedback gain of the SQUID electronics. Recently, we carried out the first beam test of the HTS SQUID monitor which was installed in the beam transport line for the ECR (electron cyclotron resonance) ion source in the CNS experimental hall. After the measurement was successfully carried out in the CNS, we installed the system into the beam transport line (E1 experimental hall) of the RIKEN Ring Cyclotron (RRC) (Figure 6) to measure the current of the high-energy heavy-ion beam which has a bunched microstructure. Figure 7 shows the measured signals of the HTS SQUID monitor (above) and those of the Faraday cup monitor (below) where a  $7 \mu\text{A}$   $\text{H}^+$  beam (10 keV) (a) and a  $600 \text{ nA}$   ${}_{40}\text{Ar}^{17+}$  beam (95 MeV/u) (b) were used.

Because the fluctuation of the measured ion beam current was 400 nA (standard deviation), an improvement of the detection resolution by more than two orders of magnitude is required. From the viewpoint of the required

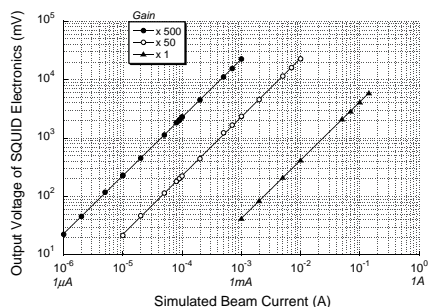


Figure 5: Plotted output voltage of the SQUID electronics as a function of the simulated beam current.

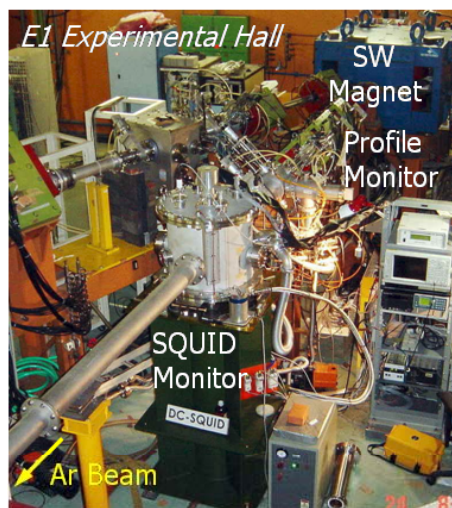


Figure 6: Beam transport line (E1 experimental hall) of the RIKEN Ring Cyclotron (RRC).

efficiency of transferring the magnetic field produced by beams to a SQUID, the efficiency of the HTS SQUID monitor is inadequate. To improve the coupling efficiency between the input coil of the SQUID and the magnetic flux induced by the current, we are investigating the possibility of fabricating the HTS coil at the bridge circuit, and introducing a high-permeability core into the SQUID chip. In addition, it was discovered that the beam position can be measured by dividing the current sensor into two parts and setting a SQUID on each bridge. Namely, it is possible to measure the beam current and beam position simultaneously in real time.

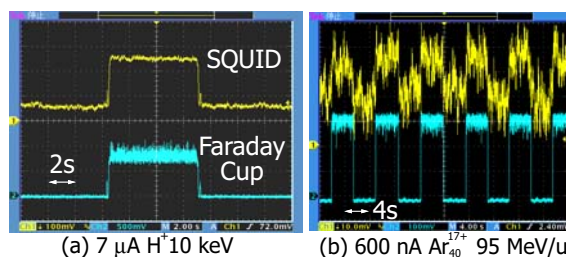


Figure 7: Measured signals of HTS SQUID monitor (above) and those of the Faraday cup monitor (below) where a  $7 \mu\text{A}$   $\text{H}^+$  beam (10 keV) (a) and a  $600 \text{ nA}$   ${}_{40}\text{Ar}^{17+}$  beam (95 MeV/u) (b) were used.

## REFERENCES

- [1] M.I. Faley et al. 2001 IEEE Trans. on Appl. Supercond. (ASC2000) 11 p 1383.
- [2] Model BMS-G with HTG-10R manufactured by TRISTAN TECHNOLOGIES.
- [3] Y. Ishikawa et al. 1992 Proc. 4th ISS'91 p 1073.
- [4] S. Watanabe et al. 2002 Proc. 8th European Particle Acc. Conf. p 1992.
- [5] Vector Fields Inc. UK.
- [6] T. Watanabe et al. 2002 Proc. 8th European Particle Accel. Conf. 2002 p 1995.
- [7] T. Watanabe et al. Supercond. Sci. and Technol. 17 2004 S450.